

# Monodisperse Iron Oxide Nanoparticles Embedded in Mg–Al Hydrotalcite as a Highly Active, Magnetically Separable, and Recyclable Solid Base Catalyst

Shun Nishimura, Atsushi Takagaki, and Kohki Ebitani\*

School of Materials Science, Japan Advanced Institute of Science and Technology, 1-1 Asahidai, Nomi 923-1292

Received March 3, 2010; E-mail: ebitani@jaist.ac.jp

Magnetically separable Mg–Al hydrotalcite was prepared by titration method in various molar ratios of (Mg + Al) to Fe, and we compared their catalytic behavior for epoxidation of 2-cyclohexen-1-one using hydrogen peroxide. The catalyst was characterized using X-ray diffraction (XRD), transmission electron microscopy (TEM), superconducting quantum interference device (SQUID), and inductively coupled plasma (ICP). The FeHT100 (ratio of (Mg + Al) to Fe = 100) showed high activity and selectivity in epoxidation of 2-cyclohexen-1-one with hydrogen peroxide. After magnetic separation, FeHT100 kept superior properties and could be reused for four reactions without loss of activity.

Progress in nanomaterials over the last few decades has afforded plenty of opportunities for the development of novel classes of heterogeneous catalysts.<sup>1–4</sup> Magnetic nanoparticles have attractive features including magnetic moments, coercivity, remanent magnetization, and spontaneous magnetism, and these properties have been applied in high-density storage media, magnetic semiconductors, magnetic fluids, hyperthermia treatment, separation and purification of biomolecules, and drug delivery.<sup>5–9</sup> From the viewpoint of catalysis, magnetic properties can serve in effective separation protocols. In order to attempt separation and recovery of catalysts from reaction products, a large amount of energy and costs are consumed for reactor maintenance. Creating the catalysts with inherent magnetic properties could lead to simpler and more environmentally benign separation.

Magnetic separation is a fascinating methodology for catalysts such as heteropoly acid,<sup>10</sup> metal complex,<sup>11–13</sup> basic ion liquid,<sup>14,15</sup> and sulfonic- or amine-functionalized nanocatalysts.<sup>16,17</sup> Although these highly active catalysts are generally homogeneous or nanosized heterogeneous, which are difficult to separate, they become easy to collect when magnetic. Moreover, separation of solid and solid catalyst can be achieved if one possesses magnetic properties, which is beneficial for one-pot synthesis using two kinds of solid catalysts.<sup>18,19</sup> There are currently many examples of magnetized solid catalysts for oxidation,<sup>20–22</sup> hydrogenation,<sup>23–25</sup> coupling,<sup>26,27</sup> hydrolysis,<sup>28</sup> esterification,<sup>29</sup> and photocatalytic reaction.<sup>30</sup> The importance of magnetic separation is rising along with extending the utilization and development of catalysts. Especially, magnetically separable acid and base catalysts are not well understood in spite of many reports of magnetically separable metal catalysts.

Layered double hydroxide clays (LDHs), which are represented by a general formula of  $[M^{2+}_{1-x}M^{3+}_x(OH)_2]^{x+}A^{n-}_{x/n} \cdot mH_2O$  where  $M^{2+}$  and  $M^{3+}$  are di- and trivalent metal ions and  $A^{n-}$  indicates the interlayer anions, show extensive applica-

tions as anion or cation exchangers,<sup>31,32</sup> adsorbents,<sup>33–35</sup> stabilizers of pigment,<sup>36</sup> and reservoirs for drugs and biomolecules.<sup>37,38</sup> In particular, hydrotalcite, which is the most well-known LDH, has been frequently used as a solid base catalyst for aldol condensation,<sup>39–41</sup> transesterification,<sup>42,43</sup> and epoxidation.<sup>44,45</sup> Recently, Duan and co-workers reported that magnetic Mg–Al–OH–LDH stabilized on  $CoFe_2O_4$  or  $MgFe_2O_4$  acted as solid base catalyst for self-condensation of acetone, where magnetic oxide was synthesized by conventional coprecipitation method.<sup>46,47</sup> However, Duan et al. did not discuss the effect of magnetic properties on the catalysis of hydrotalcite. It is important for developing an effective magnetically separable base catalyst to clarify the influence of the additive on hydrotalcite.

In this report, we have designed a magnetic hydrotalcite catalyst by using monodisperse magnetic Fe oxide nanoparticles (mono-FeNPs), and examined its usefulness as a separable and reusable solid base catalyst. The use of monodisperse magnetic nanoparticles, which have controllable magnetism, size, and solvent affinity,<sup>9,48</sup> affords clear observation of morphological change and the influence of the addition of magnetic properties to the prepared nanocomposite catalyst.

## Experimental

**Materials.** Sodium oleate was purchased from Tokyo Chemical Industry Co. Tetramethylammonium hydroxide,  $Mg(NO_3)_2 \cdot 6H_2O$ ,  $Al(NO_3)_3 \cdot 9H_2O$ ,  $Na_2CO_3 \cdot 10H_2O$ ,  $FeCl_2 \cdot 4H_2O$ ,  $FeCl_3 \cdot 6H_2O$ , and  $NH_4$  aqua were supplied by Wako Pure Chemicals. Ethanol, hexane, and NaOH were obtained from Kanto Chem. Co. Oleic acid and Amberlyst-15 were supplied by Aldrich Inc.

**Preparation of Monodispersed  $Fe_3O_4$  Nanoparticles.** Mono-FeNPs were synthesized by thermal decomposition of Fe–oleate complex according to a previous report<sup>49</sup> with some modification. First, Fe–oleate complex was prepared by refluxing  $FeCl_3 \cdot 6H_2O$  (20 mmol) and sodium oleate (60 mmol)

in a mixed solvent composed of hexane (70 mL), distilled water (30 mL), and ethanol (40 mL). Next, the formed Fe-oleate complex (6 mmol) was mixed with oleic acid (3 mmol) and tri-*n*-octylamine (82 mmol) at room temperature. Finally, the mixture was decomposed by heating at 643 K, and mono-FeNPs stabilized by oleic acid were formed. After the procedure, the hydrophobic mono-FeNPs capped with oleic acid were dispersed in tetramethylammonium hydroxide solution to make the nanoparticles hydrophilic.

**Preparation of Magnetic Mg–Al Hydrotalcite.** Magnetic Mg–Al hydrotalcite with  $\text{Fe}_3\text{O}_4$  was prepared by coprecipitation method.  $\text{Mg}(\text{NO}_3)_2 \cdot 6\text{H}_2\text{O}$  (12.5 mmol),  $\text{Al}(\text{NO}_3)_3 \cdot 9\text{H}_2\text{O}$  (2.5 mmol), and synthesized mono-FeNPs were dispersed in 100 mL of water. Water solution containing both NaOH and  $\text{Na}_2\text{CO}_3$  ( $\text{NaOH}/\text{Na}_2\text{CO}_3 = 2$ ) was slowly added dropwise into the above solution until pH ca. 10 under vigorous stirring. The resulting solution was aged at 333 K for 2 h, then filtered, washed with water, and dried at 373 K overnight. Synthesized magnetic Mg–Al hydrotalcite with  $\text{Fe}_3\text{O}_4$  is described as FeHTX, where X denotes the (Mg + Al)/Fe molar ratio of each sample used. As a comparison, pure hydrotalcite (HT) was prepared using a similar method.

**Preparation of Coprecipitated  $\text{Fe}_3\text{O}_4$ .** Both  $\text{FeCl}_2 \cdot 4\text{H}_2\text{O}$  (3.7 mmol) and  $\text{FeCl}_3 \cdot 6\text{H}_2\text{O}$  (7.4 mmol) were dissolved in 180 mL water, and 4 M  $\text{NH}_4$  water solution was added dropwise into the above solution until pH ca. 10. After the resulting precipitate was aged for 2 h at 333 K, it was filtered, washed, and dried at room temperature.

**Preparation of HT Containing Mono-FeNPs by Adsorption Method.** The prepared HT and the synthesized mono-FeNPs were stirred together in 50 mL  $\text{H}_2\text{O}$  for 8 h at room temperature. Then, the mixture was filtered, washed, and dried at room temperature.

**Characterizations.** Powder X-ray diffraction (XRD) patterns were obtained with a Rigaku RINT2000 X-ray diffractometer using  $\text{Cu K}\alpha_1$  radiation ( $\lambda = 0.154$  nm) and a power of 40 kV and 20 mA. The morphologies of samples were observed by transmission electron microscopy (TEM, HITACHI H-7100). Magnetic properties were measured by superconducting quantum interference device (SQUID, Quantum Design MPMS-XL) ranging from  $-5.0$  to  $5.0$  T. The concentrations of Fe for each FeHTX catalysts were determined by an inductively coupled plasma (ICP, Shimadzu ICPS-7000).

**Epoxidation of 2-Cyclohexen-1-one Using Hydrogen Peroxide.** The reaction was carried out in a Schlenk-flask in methanol solvent at 313 K for 4 h under a flow of  $\text{N}_2$ . After the reaction, the catalyst was washed with 30 mL acetone twice, dried at 353 K overnight, and reused for further reaction. A gas chromatograph (GC) with a capillary column (TC-FFAP, 0.25 mm  $\times$  30 m), was used to analyze the products.

**A One-Pot Synthesis of 5-Hydroxymethylfurfural (HMF) from Glucose.** The reaction was performed at 373 K for 3 h in 3 mL of *N,N*-dimethylformamide using 0.05 g of magnetic hydrotalcite and 0.1 g of Amberlyst-15. High-performance liquid chromatography (HPLC) using a Bio-rad Aminex HPX-87H column was used to analyze the products.

## Results and Discussion

**Crystal Structure.** X-ray diffraction (XRD) patterns for

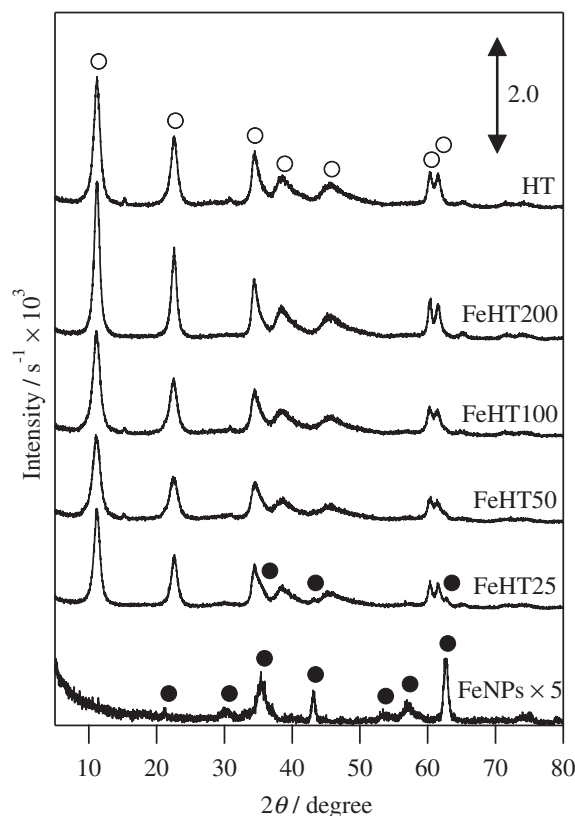


**Figure 1.** XRD patterns for HT, FeHTXs, and mono-FeNPs. (○) Hydrotalcite phase, (●) magnetite phase.

HT, FeHTXs, and mono-FeNPs are shown in Figure 1. Mono-FeNPs shows magnetite ( $\text{Fe}_3\text{O}_4$ ) phase, and the crystal size was  $D_{311} = 7.3$  nm calculated by Scherrer's equation. Prepared HT exhibited clear peaks of hydrotalcite-like LDHs at  $2\theta$  angles of 11.2, 22.6, 34.5, 38.0, 45.7, 60.3, and 61.5° corresponding to (003), (006), (012), (015), (018), (110), and (113) reflections, respectively, and basal spacing  $d_{003}$  is 0.79 nm. All diffraction patterns and basal spacing of FeHTXs were similar to those of HT. For FeHTXs, small peaks around at  $2\theta$  angles of 35.5, 42.9, and 62.7 attributed to a magnetite phase were observed, depending on the amount of mono-FeNPs. These results indicated that HT was formed even in the presence of mono-FeNPs, and the mono-FeNPs had little effect on the structure of HT.

**Structural Morphology.** Transmission electron microscope (TEM) images of mono-FeNPs, FeHT25, FeHT100, and HT are shown in Figure 2. Mono-FeNPs are highly mono-disperse nanoparticles, with about 20.0 nm average diameter (Figure 2a) and narrow size distributions (inset Figure 2). These morphologies were similar to those reported in the literature.<sup>49</sup> The TEM image of HT (Figure 2d) shows the plate-like morphology which is characteristic of LDH materials.<sup>50–52</sup> Moreover, for both FeHT25 (Figure 2b) and FeHT100 (Figure 2c), the formation of nanocomposite where mono-FeNPs were embedded in plate-like hydrotalcite was observed, indicating that FeHTXs could be prepared without changing the morphologies of hydrotalcite or mono-FeNPs.

**Magnetic Properties.** In order to evaluate magnetic properties, magnetization curves were measured by a super-

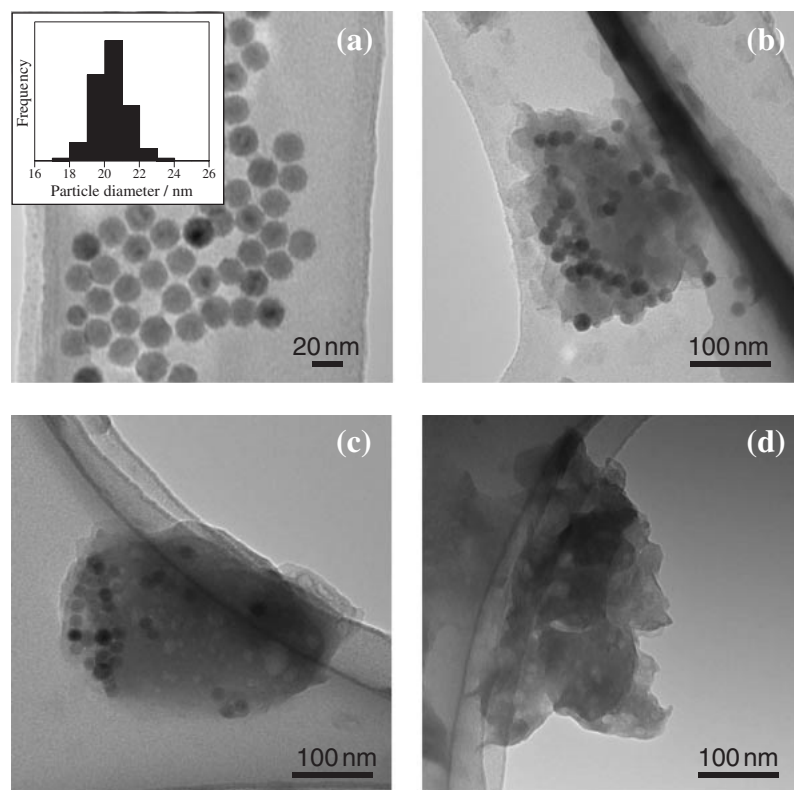


**Figure 2.** TEM images of (a) mono-FeNPs, (b) FeHT25, (c) FeHT100, and (d) HT. Inset shows size distribution of the mono-FeNPs.

conducting quantum interference device (SQUID). Figure 3 shows magnetization curves for mono-FeNPs at 10 and 300 K. The magnetization of mono-FeNPs drastically increased under a low external magnetic field, and was saturated under 5 T without hysteresis at 300 K. At 10 K, the same behavior was obtained with hysteresis, corresponding to strong soft magnetic behavior. These magnetization curves of mono-FeNPs exhibited superparamagnetic behavior, and the saturation magnetization was  $46.0 \text{ emu g}^{-1}$  at 10 K and  $44.6 \text{ emu g}^{-1}$  at 300 K. The magnetization curves for FeHTXs and HT at 10 and 300 K are shown in Figure 4. The case of HT shows slight negative magnetization, and intensity decreased with increasing external magnetic field regardless of measurement temperature. All the FeHTXs displayed similar magnetic curves to that of mono-FeNPs, and they exhibited superparamagnetic behavior with hysteresis at 10 K and without at 300 K. All magnetizations of FeHTXs were saturated at approximately 0.5 T at 300 K. These magnetizations of FeHTXs under 0.5 T, which is a similar condition to catalyst separation using a Nd–Fe–B magnet (vide infra), were 2.0 (FeHT25), 0.95 (FeHT50), 0.46 (FeHT100), and 0.20 (FeHT200)  $\text{emu g}^{-1}$ , respectively. Compared with mono-FeNPs, FeHTXs had a smaller amount of magnetization. These tendencies show the saturated magnetizations of FeHTXs were directly related to the amounts of mono-FeNPs. Meanwhile, at fields above 0.5 T, their magnetizations gradually diminished. These tendencies suggest that the decrease of magnetization for FeHTXs after saturation was due to the diamagnetic properties of HT. These results indicate that FeHTXs present magnetic properties of both superparamagnetism (derived from mono-FeNPs), and diamagnetism (from hydrotalcite).

**Table 1.** Epoxidation of 2-Cyclohexen-1-one Using Hydrogen Peroxide in Methanol<sup>a)</sup>

Catalyst	Fe concentration <sup>b)</sup> /wt %	Yield <sup>c)</sup> /%	Selectivity /%
HT	—	95	97
FeHT200	0.28	81	89
FeHT100	0.53	80	91
FeHT50	1.29	77	92
FeHT25	2.99	52	77
Fe <sub>3</sub> O <sub>4</sub> <sup>d)</sup>	—	4	—
Blank	—	0	0

a) Reaction conditions: 2-cyclohexen-1-one (2 mmol), catalyst (0.15 g), 30% aq. H<sub>2</sub>O<sub>2</sub> (8 mmol), methanol (5 mL), 313 K, 4 h. b) Calculated by ICP analyzer using a calibration curve. c) Determined by GC using naphthalene (0.05 mmol) as an internal standard. d) Prepared by titration method.

**The Amount of Fe on the FeXHT Catalysts.** The Fe concentrations of each FeHTX catalysts are shown in Table 1. FeHT200 contains 0.28 wt % Fe, and the concentrations gradually increased as the amounts of additive mono-FeNPs, 0.53 (FeHT100), 1.29 (FeHT50), and 2.99 (FeHT25) wt %. Using mono-FeNPs as a magnetic agent was an effective method to control the magnetization of catalyst. Additionally, it is obvious that the saturated magnetizations were related

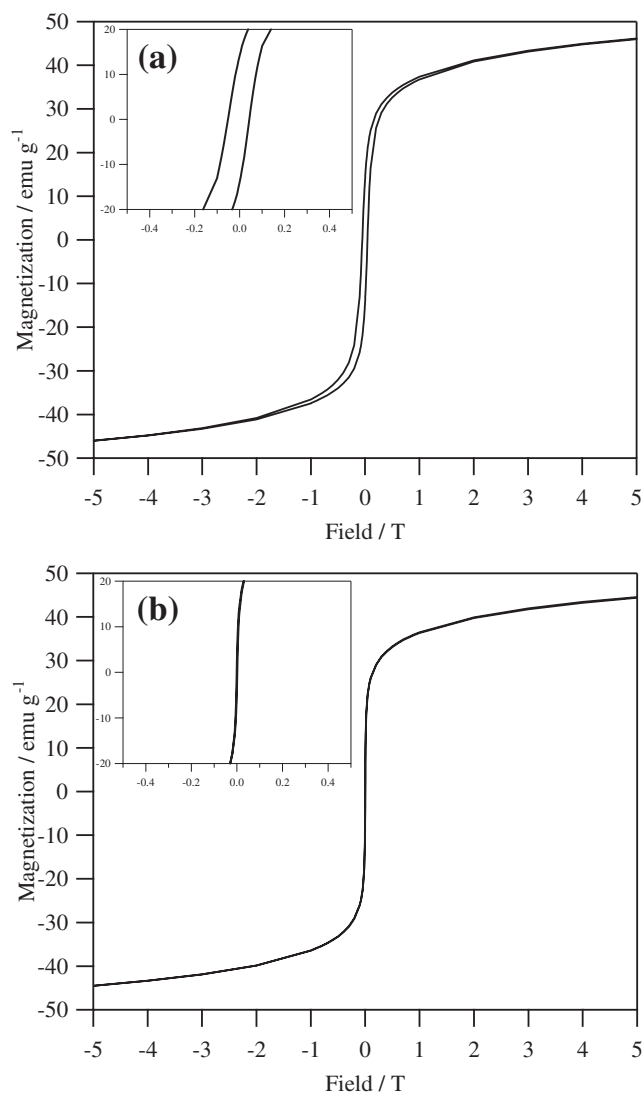


**Figure 3.** Magnetization curves for mono-FeNPs at (a) 10 and (b) 300 K. The insets emphasize details near the origin.

to the amounts of mono-FeNPs (see Supporting Information Figure S1).

**Catalytic Activity for Epoxidation of 2-Cyclohexen-1-one.** The catalytic activities for magnetic FeHTXs were evaluated for epoxidation of 2-cyclohexen-1-one using hydrogen peroxide as an oxidant. The epoxidation of  $\alpha,\beta$ -unsaturated ketones has a great impact, because the formed epoxyketones can be converted to various organic materials. This epoxidation of electro-deficient olefin using  $\text{H}_2\text{O}_2$  was traditionally performed in the presence of homogeneous base, NaOH. The results for HT and FeHTX catalysts are shown in Table 1. Without catalyst, the reaction did not proceed. In the case of using HT, the yield and selectivity for 2,3-epoxycyclohexanone were 95% and 97%, respectively. FeHT200, FeHT100, and FeHT50 exhibited high catalytic activities (ca. 80% yield and ca. 90% selectivity) without significant loss, compared with intrinsic hydrotalcite activity. Moreover, these catalysts could be simply recovered from reaction solvent using a magnetic field (Nd-Fe-B magnet of ca. 460 mT) after the reaction (Figure 5 and see Supporting Information Figure S2).

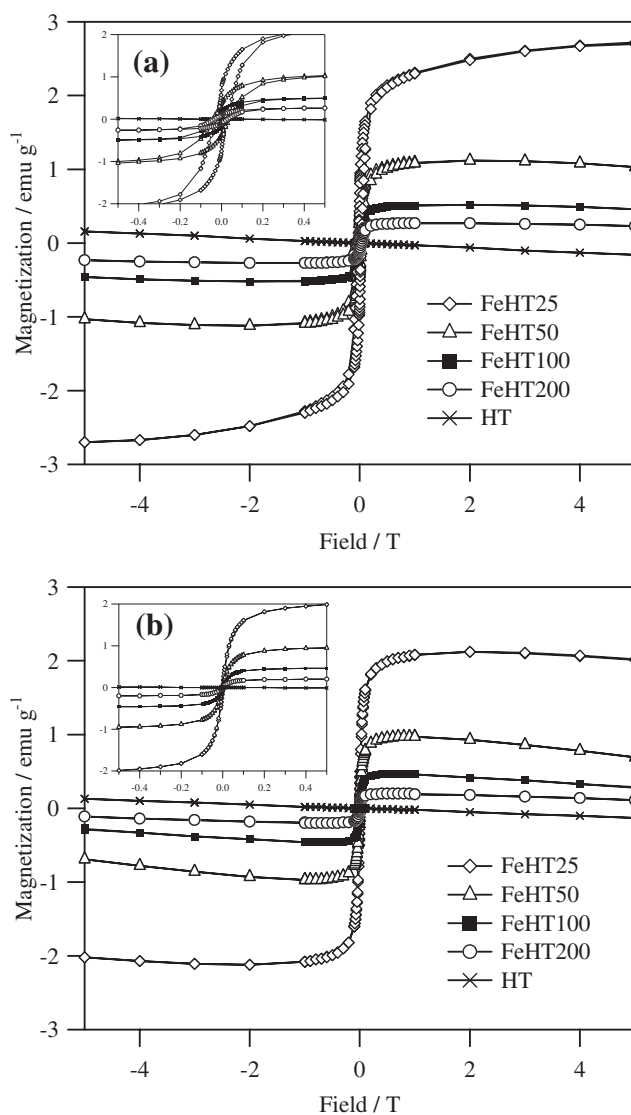


**Figure 4.** Magnetization curves for HT and FeHTXs at (a) 10 and (b) 300 K. The insets emphasize details near the origin.

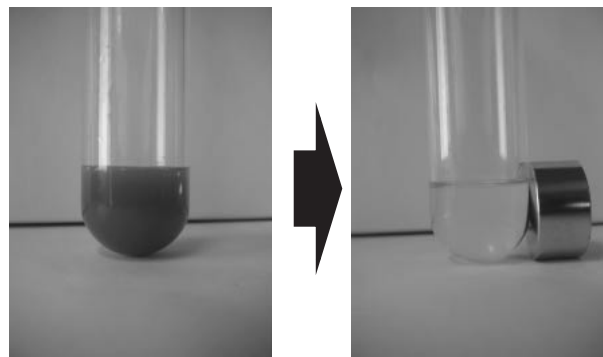


**Figure 5.** Magnetic separation after first reaction in the case of FeHT100.

To evaluate recyclability of the catalyst, the recovered HT and FeHT100 were tested for further recycle reactions. HT and FeHT100 maintained high catalytic performance and good

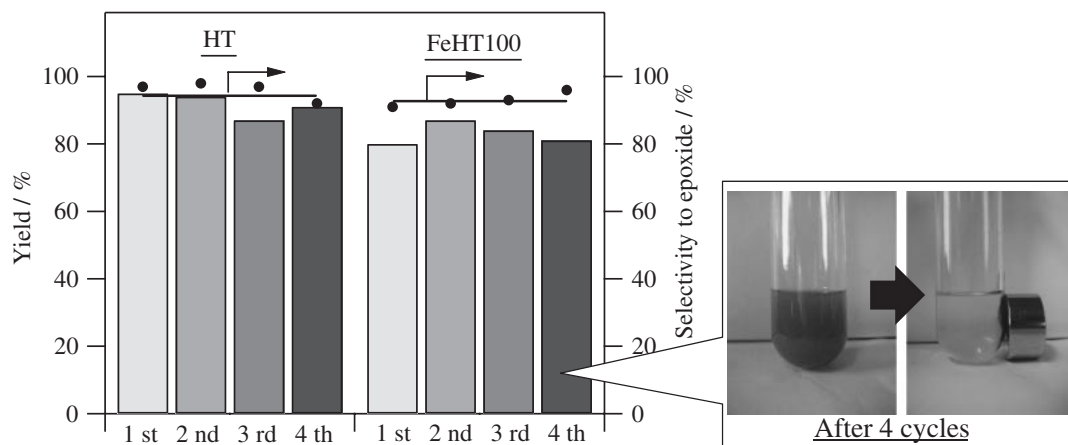


Figure 6. Recyclability of HT and FeHT100 catalysts. Photo shows case of FeHT100.

magnetic separability for at least 4 reactions for FeHT100 (Figure 6). However, the reaction using FeHT25 showed 52% yield and 77% selectivity, lower than that of other FeHTXs.  $\text{Fe}_3\text{O}_4$  nanoparticles exhibited poor activity for this reaction (4% yield). A control experiment revealed that the physical mixture of HT and coprecipitated  $\text{Fe}_3\text{O}_4$  at similar compositions as FeHT25 showed good catalytic activity (77% yield and 91% selectivity). The FeHT25 catalyst synthesized by an adsorption method (where HT and mono-FeNPs were stirred together in water solution and filtered) showed 50% yield and 89% selectivity. Furthermore, the magnetization scarcely effects on catalytic activity, because the relationships between magnetization and catalytic activity was not collated (see Supporting Information Figure S1), and the external magnetic field from magnetic stirrer was very weak under reaction condition (ca. 30 mT). Therefore, we suppose that the lower activity of FeHT25 was attributable to excess of mono-FeNPs, which acted as an inhibitor of the reaction.

**Further Catalytic Application for a One-Pot Synthesis of 5-Hydroxymethylfurfural (HMF) from Glucose.** For expanding catalytic application of magnetic HTs, FeHT100 was examined as a heterogeneous catalyst for one-pot synthesis of 5-hydroxymethylfurfural (HMF) from glucose. HMF is a material with good potential as an intermediate for various chemical materials.<sup>53</sup> HMF production from glucose is very attractive from the viewpoint of effective utilization of biomass, because glucose is the most abundant monosaccharide.<sup>54</sup> We have very recently demonstrated that HMF production from glucose can be achieved in one-pot in the presence of solid acid and solid base catalysts.<sup>55</sup> In one-pot synthesis, base catalyst isomerizes glucose to fructose, and acid catalyst dehydrates fructose to HMF, resulting in efficient production of HMF with high selectivity. Using 0.05 g HT as solid base catalyst and 0.1 g Amberlyst-15 as solid acid catalyst showed 9% yield and 30% HMF selectivity. When we used 0.05 g FeHT100 and 0.1 g Amberlyst-15, 9% yield and 28% HMF selectivity were obtained under the same conditions. After the reaction, the FeHT100 catalyst was easily separated by using a magnet, and Amberlyst-15 was quickly precipitated as shown in Figure 7. This indicated that two different solid catalysts could be separated using FeHT100, with activity comparable to HT.

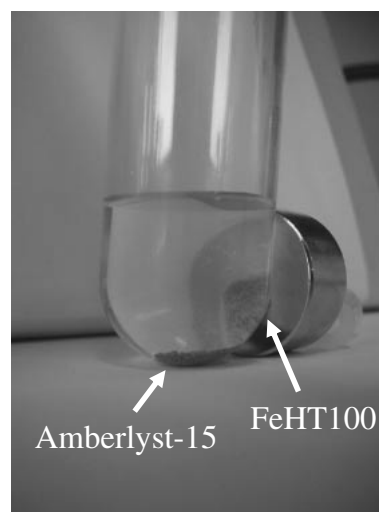


Figure 7. Magnetic separation after one-pot synthesis.

## Conclusion

In summary, we have succeeded in preparation of a highly active and separable magnetic Mg–Al hydrotalcite catalyst using mono-FeNPs. This hybrid material acted as a heterogeneous solid base and could be reused without significant loss of activity, selectivity, and magnetic properties for epoxidation of 2-cyclohexen-1-one using hydrogen peroxide. The magnetic Mg–Al hydrotalcite catalyst also showed activity and good separability for the one-pot synthesis of 5-hydroxymethylfurfural from glucose.

We thank Ms. Mary Ann Mooradian (JAIST) for her careful reading of, and useful comments about, the manuscript.

## Supporting Information

Relationships of Fe concentration, catalytic activity, and magnetization, and photographs of magnetic separation after first reaction. This material is available free of charge on the web at <http://www.csj.jp/journals/bcsj/>.

## References

- 1 X. Xie, Y. Li, Z.-Q. Li, M. Haruta, W. Shen, *Nature* **2009**, 458, 746.
- 2 Y. Lou, M. M. Maye, L. Han, J. Luo, C.-J. Zhong, *Chem. Commun.* **2001**, 473.
- 3 M. O. Nutt, J. B. Hughes, M. S. Wong, *Environ. Sci. Technol.* **2005**, 39, 1346.
- 4 R. M. Rioux, H. Song, M. Grass, S. Habas, K. Niesz, J. D. Hoefelmeyer, P. Yang, G. A. Somorjai, *Top. Catal.* **2006**, 39, 167.
- 5 S. Saita, S. Maenosono, *Chem. Mater.* **2005**, 17, 3705.
- 6 X. Gao, K. M. K. Yu, K. Y. Tam, S. C. Tsang, *Chem. Commun.* **2003**, 2998.
- 7 Z. Huang, J. Li, Q. Chen, H. Wang, *Mater. Chem. Phys.* **2009**, 114, 33.
- 8 W. Shan, T. Yu, B. Wang, J. Hu, Y. Zhang, X. Wang, Y. Tang, *Chem. Mater.* **2006**, 18, 3169.
- 9 Y. Jun, Y.-M. Huh, J. Choi, J.-H. Lee, H.-T. Song, S. Kim, S. Yoon, K.-S. Kim, J.-S. Shin, J.-S. Suh, J. Cheon, *J. Am. Chem. Soc.* **2005**, 127, 5732.
- 10 T. Goto, Y. Sakamoto, Y. Kamiya, *Chem. Lett.* **2009**, 38, 736.
- 11 C. Che, W. Li, S. Lin, J. Chen, J. Zheng, J. Wu, Q. Zheng, G. Zhang, Z. Yang, B. Jiang, *Chem. Commun.* **2009**, 5990.
- 12 A. Hu, G. T. Yee, W. Lin, *J. Am. Chem. Soc.* **2005**, 127, 12486.
- 13 T. Hirakawa, S. Tanaka, N. Usuki, H. Kanzaki, M. Kishimoto, M. Kitamura, *Eur. J. Org. Chem.* **2009**, 789.
- 14 X. Zheng, S. Luo, L. Zhang, J.-P. Cheng, *Green Chem.* **2009**, 11, 455.
- 15 Y. Zhang, Y. Zhao, C. Xia, *J. Mol. Catal. A: Chem.* **2009**, 306, 107.
- 16 C. S. Gill, B. A. Price, C. W. Jones, *J. Catal.* **2007**, 251, 145.
- 17 N. T. S. Phan, C. W. Jones, *J. Mol. Catal. A: Chem.* **2006**, 253, 123.
- 18 R. Abu-Reziq, D. Wang, M. Post, H. Alper, *Chem. Mater.* **2008**, 20, 2544.
- 19 N. T. S. Phan, C. S. Gill, J. V. Nguyen, Z. J. Zhang, C. W. Jones, *Angew. Chem., Int. Ed.* **2006**, 45, 2209.
- 20 K. Mori, K. Sugihara, Y. Kondo, T. Takeuchi, S. Morimoto, H. Yamashita, *J. Phys. Chem. C* **2008**, 112, 16478.
- 21 M. V. Barmatova, I. D. Ivanchikova, O. A. Kholdeeva, A. N. Shmakov, V. I. Zaikovskii, M. S. Mel'gunov, *J. Mater. Chem.* **2009**, 19, 7332.
- 22 K. Mori, S. Kanai, T. Hara, T. Mizugaki, K. Ebitani, K. Jitsukawa, K. Kaneda, *Chem. Mater.* **2007**, 19, 1249.
- 23 J. Zhang, Y. Wang, H. Ji, Y. Wei, N. Wu, B. Zuo, Q. Wang, *J. Catal.* **2005**, 229, 114.
- 24 M. J. Jacinto, O. H. C. F. Santos, R. F. Jardim, R. Landers, L. M. Rossi, *Appl. Catal., A* **2009**, 360, 177.
- 25 D. K. Yi, S. S. Lee, J. Y. Ying, *Chem. Mater.* **2006**, 18, 2459.
- 26 H. Yoon, S. Ko, J. Jang, *Chem. Commun.* **2007**, 1468.
- 27 Z. Wang, P. Xiao, B. Shen, N. He, *Colloids Surf., A* **2006**, 276, 116.
- 28 J. L. Rodgers, J. W. Rathke, R. J. Klinger, C. L. Marshall, *Catal. Lett.* **2007**, 114, 145.
- 29 Q. Wang, W. Zhao, X. Sun, W. Zhao, *Catal. Lett.* **2008**, 121, 324.
- 30 L. Li, Y. Feng, Y. Li, W. Zhao, J. Shi, *Angew. Chem., Int. Ed.* **2009**, 48, 5888.
- 31 F. Millange, R. I. Walton, L. Lei, D. O'Hare, *Chem. Mater.* **2000**, 12, 1990.
- 32 M. Meyn, K. Beneke, G. Lagaly, *Inorg. Chem.* **1993**, 32, 1209.
- 33 J. Inacio, C. Taviot-Gu  ho, C. Forano, J. P. Besse, *Appl. Clay Sci.* **2001**, 18, 255.
- 34 M. Jos   dos Reis, F. Silv  rio, J. Tronto, J. B. Valim, *J. Phys. Chem. Solids* **2004**, 65, 487.
- 35 Q. Hu, Z. Xu, S. Qiao, F. Haghsheer, M. Wilson, G. Q. Lu, *J. Colloid Interface Sci.* **2007**, 308, 191.
- 36 Y. Kohno, K. Totsuka, S. Ikoma, K. Yoda, M. Shibata, R. Matsushima, Y. Tomita, Y. Maeda, K. Kobayashi, *J. Colloid Interface Sci.* **2009**, 337, 117.
- 37 J.-H. Choy, S.-Y. Kwak, Y.-J. Jeong, J.-S. Park, *Angew. Chem., Int. Ed.* **2000**, 39, 4041.
- 38 H. Zhang, D. Pan, K. Zou, J. He, X. Duan, *J. Mater. Chem.* **2009**, 19, 3069.
- 39 Z. An, W. Zhang, H. Shi, J. He, *J. Catal.* **2006**, 241, 319.
- 40 H. C. Greenwell, P. J. Holliman, W. Jones, B. V. Velasco, *Catal. Today* **2006**, 114, 397.
- 41 D. Tichit, M. N. Bennani, F. Figueras, R. Tessier, J. Kervennal, *Appl. Clay Sci.* **1998**, 13, 401.
- 42 E. Li, Z. P. Xu, V. Rudolph, *Appl. Catal., B* **2009**, 88, 42.
- 43 B. M. Choudary, M. L. Kantam, C. V. Reddy, S. Aranganathan, P. L. Santhi, F. Figueras, *J. Mol. Catal. A: Chem.* **2000**, 159, 411.
- 44 K. Yamaguchi, K. Mori, T. Mizugaki, K. Ebitani, K. Kaneda, *J. Org. Chem.* **2000**, 65, 6897.
- 45 T. Honma, M. Nakajo, T. Mizugaki, K. Ebitani, K. Kaneda, *Tetrahedron Lett.* **2002**, 43, 6229.
- 46 H. Zhang, R. Qi, D. G. Evans, X. Duan, *J. Solid State Chem.* **2004**, 177, 772.
- 47 Y. Xu, H. Zhang, X. Duan, Y. Ding, *Mater. Chem. Phys.* **2009**, 114, 795.
- 48 S. Alam, C. Anand, K. Ariga, T. Mori, A. Vinu, *Angew. Chem., Int. Ed.* **2009**, 48, 7358.
- 49 J. Park, K. An, Y. Hwang, J.-G. Park, H.-J. Noh, J.-Y. Kim, J.-H. Park, N.-M. Hwang, T. Hyeon, *Nat. Mater.* **2004**, 3, 891.
- 50 F. Winter, A. J. van Dillen, K. P. Jong, *Chem. Commun.* **2005**, 3977.
- 51 P. Benito, I. Guinea, F. M. Labajos, V. Rives, *J. Solid State Chem.* **2008**, 181, 987.
- 52 F. Delorme, A. Seron, M. Bizi, V. Jean-Prost, D. Martineau, *J. Mater. Sci.* **2006**, 41, 4876.
- 53 Y. Rom  n-Leshkov, C. J. Barrett, Z. Y. Liu, J. A. Dumesic, *Nature* **2007**, 447, 982.
- 54 H. Zhao, J. E. Holladay, H. Brown, Z. C. Zhang, *Science* **2007**, 316, 1597.
- 55 A. Takagaki, M. Ohara, S. Nishimura, K. Ebitani, *Chem. Commun.* **2009**, 6276.